Renewable Energy 218 (2023) 119357

Contents lists available at ScienceDirect

Renewable Energy

journal homepage: www.elsevier.com/locate/renene

Wind power forecasting based on hybrid CEEMDAN-EWT deep learning method

Irene Karijadi [a,c,*], Shuo-Yan Chou [a,b], Anindhita Dewabharata [a,b]

[a] Department of Industrial Management, National Taiwan University of Science and Technology, Taipei, Taiwan
[b] Taiwan Building Technology Center, National Taiwan University of Science and Technology, Taipei, Taiwan
[c] Department of Industrial Engineering, Widya Mandala Catholic University, Surabaya, Indonesia

ARTICLE INFO

Keywords:
Wind power
Forecasting
Deep learning
Long short term memory
Data preprocessing
Artificial Intelligence

ABSTRACT

A precise wind power forecast is required for the renewable energy platform to function effectively. By having a precise wind power forecast, the power system can better manage its supply and ensure grid reliability. However, the nature of wind power generation is intermittent and exhibits high randomness, which poses a challenge to obtaining accurate forecasting results. In this study, a hybrid method is proposed based on Complete Ensemble Empirical Mode Decomposition with Adaptive Noise (CEEMDAN), Empirical Wavelet Transform (EWT), and deep learning-based Long Short-Term Memory (LSTM) for ultra-short-term wind power forecasting. A combination of CEEMDAN and EWT is used as the preprocessing technique, where CEEMDAN is first employed to decompose the original wind power data into several subseries, and the EWT denoising technique is used to denoise the highest frequency series generated from CEEMDAN. Then, LSTM is utilized to forecast all the subseries from the CEEMDAN-EWT process, and the forecasting results of each subseries are aggregated to achieve the final forecasting results. The proposed method is validated on real-world wind power data in France and Turkey. Our experimental results demonstrate that the proposed method can forecast more accurately than the benchmarking methods.

1. Introduction

The global energy demand is projected to grow by 48% within the next twenty years due to the rapid increase in the global population [1]. However, fossil fuels as the current primary sources of energy supply [2] are limited. The increased use of fossil fuels combined with supply limits has resulted in higher energy prices and scarcities [3]. Hence, renewable energy sources have been gaining much attention in recent years as alternative energy sources to replace conventional fossil fuels [4]. There has been a global shift to adopt renewable energy sources to reduce our dependence on fossil fuels and mitigate the risk of global warming [5]. Renewable energy sources, combined with energy efficiency improvements, are able to reduce energy-related CO^2 emissions by over 90%, which can form a viable climate solution [6]. Therefore, the share of renewable energy in the global primary energy supply is predicted to rise from 14% in 2015 to 63% by the year 2050 [7]. Among the renewable energy sources, the wind energy sector is one of the fastest-growing renewable energy sources [8,9]. Its attractiveness has grown because of its significant cost reduction [10] and it is easier to install on a large scale compared to other renewable energy sources such as solar and tidal energy [11].

Despite its advantages, wind energy is accompanied by some challenges. Wind energy is highly influenced by nature. Therefore, the output generated by wind power is highly intermittent and unsteady [12]. These characteristics can introduce some technical issues, such as grid interconnection, power reliability, and generation control [12], which can increase the vulnerability of power systems [13]. To improve the efficiency and reliability of wind power generation, researchers have proposed various optimal control strategies and modeling techniques for wind turbines [14–16]. For example, Kong et al. [15] proposed a distributed economic model predictive scheme that integrates the power tracking and economic optimization of the wind farm. Abdelbaky et al. [16] proposed wind turbine collective pitch control strategies based on fuzzy modeling.

Wind power forecasting is also crucial for managing the variability and uncertainty of wind power, enabling power systems to make informed decisions on power generation, storage, and dispatch. By understanding wind power predictability and its fluctuations, the power

* Corresponding author. Department of Industrial Management, National Taiwan University of Science and Technology, Taipei, Taiwan.
E-mail address: irenekarijadi92@gmail.com (I. Karijadi).

https://doi.org/10.1016/j.renene.2023.119357
Received 20 October 2022; Received in revised form 10 July 2023; Accepted 22 September 2023
Available online 22 September 2023

system can optimally manage its operation and maintain its reliability. Thus, precise wind power forecasting is critical for the reliability and efficiency of power systems that integrate wind energy resources [17].

Wind power forecasting can be categorized based on the forecasting horizon into ultra-short-term (a few seconds to 4 h ahead), short-term (4 h to one day ahead), medium-term (one day to one week ahead), and long-term forecasting (more than one week) [18]. Ultra-short-term forecasts provide valuable information to help decision-makers optimize load tracking and turbine control; short-term forecasts are mainly used for preload sharing, and medium and long-term forecasts are generally for maintenance scheduling [19]. Due to the rising penetration levels of wind power into the grid, it is important to have a more accurate forecast of wind power generation with lead times of a few minutes ahead, since grid operators need to maintain grid stability [20]. Furthermore, compared to other wind power forecasts, the ultra short-term wind power forecast requires more precise results and it is more difficult to forecast due to its shorter time frames [21]. This study focuses on enhancing the accuracy of ultra-short-term wind power forecasting.

Accurate wind power forecasts bring significant economic impacts and technical advantages [22]. Hence, several approaches have been developed by researchers for the development and improvement of wind power forecasting, including statistical methods such as auto-regressive integrated moving average (ARIMA) [23] and artificial intelligence methods including Artificial Neural Network (ANN) [24,25], Support Vector Regression (SVR) [26,27] and Random Forest (RF) [28]. Recently, the application of deep learning methods such as Long Short-Term Memory (LSTM) has also become increasingly popular in the field of wind power forecasting due to its superior forecasting ability in dealing with complex nonlinear data [29] and its capability to effectively capture information in time series data [30]. In Ref. [31], LSTM is utilized to forecast wind power generation and the results demonstrate that LSTM has higher forecasting accuracy compared to other traditional artificial intelligence methods such as SVM.

Wind power data exhibits high randomness and high volatility owing to the intermittent nature of wind energy [32]. Due to its randomness and high volatility characteristics, it is quite challenging to obtain a precise wind power forecasting result using a single forecasting method alone. Therefore, some researchers proposed to use hybrid methods by combining artificial intelligence methods with data preprocessing strategies. The decomposition-based method is now one of the most extensively used data preprocessing methods and it has produced good forecasting results [33]. In the decomposition-based hybrid methods, the decomposition techniques will be used to decompose original wind data into several more relatively stationary subseries. Then a forecasting model will be built for each subseries and the forecasting results are added together to obtain the final forecasting results. By decomposing into several more relatively stationary subseries and forecasting each subseries individually, it can effectively enhance the accuracy of wind forecasting.

Several decomposition-based hybrid methods have been employed in the field of wind power forecasting, such as Empirical Mode Decomposition [34,35], Ensemble Empirical Mode Decomposition (EEMD) [36], Complementary EEMD (CEEMD) [37,38], and Complete Ensemble Empirical Mode Decomposition with Adaptive Noise (CEEMDAN) [39–41]. The experimental results showed that decomposition-based hybrid methods have been proven to be effective in increasing forecasting accuracy and superior compared to individual models. For instance, Wang et al. [35] utilized EMD as a data decomposition method and combined it with Elman Neural Network (ENN) to forecast wind speed. The EMD is used to decompose the original data and ENN is utilized to build the forecasting models for each subseries. Their results concluded that the EMD-ENN can be used to improve the forecasting accuracy of wind speed. Hu et al. [38] proposed a hybrid method based on EEMD decomposition for wind speed forecasting. In their method, the original time series is decomposed into several components by using EEMD, and LSTM is used to predict each component. In addition, Bayesian Optimization (BO) is utilized to fine-tune the hyperparameters of LSTM. Ren et al. [42] employed EMD and its improved version to decompose wind data and used ANN and SVR to build the forecasting methods. Their study showed that CEEMDAN had better performance compared to EMD, EEMD, and CEEMD [42].

Although there has been a significant improvement achieved by combining the decomposition technique with the artificial intelligence method, further improvement is still needed to improve the accuracy of wind power forecasting. Considering the highest frequency series produced by the CEEMDAN decomposition technique still exhibits high volatility and contains noises [43]. The highest frequency series is the most difficult series to forecast [44] and it may deteriorate the forecasting accuracy. Most wind power forecasting methods typically only rely on a single data decomposition method for processing without considering the highest frequency problem. For instance, Wang et al. [35] solely employed EMD for data decomposition while Hu et al. [38] exclusively utilized EEMD. As a result, the forecasting accuracy is limited due to the complexity of the highest frequency series is not appropriately handled. The highest frequency series problem could be tackled by applying Empirical Wavelet Transform (EWT) denoising technique to the highest frequency series generated from CEEMDAN. Since IMF 1 as the highest frequency series is the most irregular subseries and exhibits high randomness, the EWT denoising technique can be used to reduce the randomness and remove the noise in the input data of IMF 1 and thus further improve the forecasting accuracy. EWT is a signal processing technique and it has capabilities for eliminating noise and unrelated information in the data [45]. EWT has demonstrated excellent performance in various applications such as fault diagnosis [46], electrocardiogram (ECG) signals denoising [47], and seismic data analysis [48]. Several researchers have also made some attempts to employ EWT for denoising wind data. For instance, Refs. [49–51] employed EWT to eliminate the noise in the wind speed data. The EWT method can represent the original data into several modes and screen out the noisy residuals [51] and by utilizing EWT to denoise the original data, the forecasting quality of the wind speed can be improved.

Based on the abovementioned issues, this study proposes an ultra-short-term wind power forecasting method using a new hybrid CEEMDAN-EWT deep learning LSTM method. First, CEEMDAN transforms the original wind power data into several subseries. Then, EWT is used to denoise the highest frequency series generated from CEEMDAN. Reducing the noise in the highest frequency series could further reduce the forecasting difficulty. After CEEMDAN-EWT data preprocessing, each of the subseries is forecasted individually by utilizing LSTM. In the final stage, the forecasting results of each subseries are added together to achieve the final forecasting results. The combination of the CEEMDAN decomposition, EWT denoising technique, and LSTM has not been presented in the field of ultra-short-term wind power forecasting before, to the best of our knowledge. The remainder of this paper is structured as follows. Section 2 briefly reviews the background theory of the proposed method. Section 3 describes the framework of the proposed method. The experimental part is covered in Section 4. Finally, Section 5 concludes the paper and discusses future research directions.

2. Theoretical background

In this section, the theoretical backgrounds of the methods involved in our proposed method are described in detail.

2.1. Complete Ensemble Empirical Mode Decomposition with Adaptive Noise (CEEMDAN)

Complete Ensemble Empirical Mode Decomposition with Adaptive Noise (CEEMDAN) is a signal processing method that can decompose nonlinear and nonstationary data into several Intrinsic Mode Functions (IMF) series, which are more stable and stationary. CEEMDAN is built on

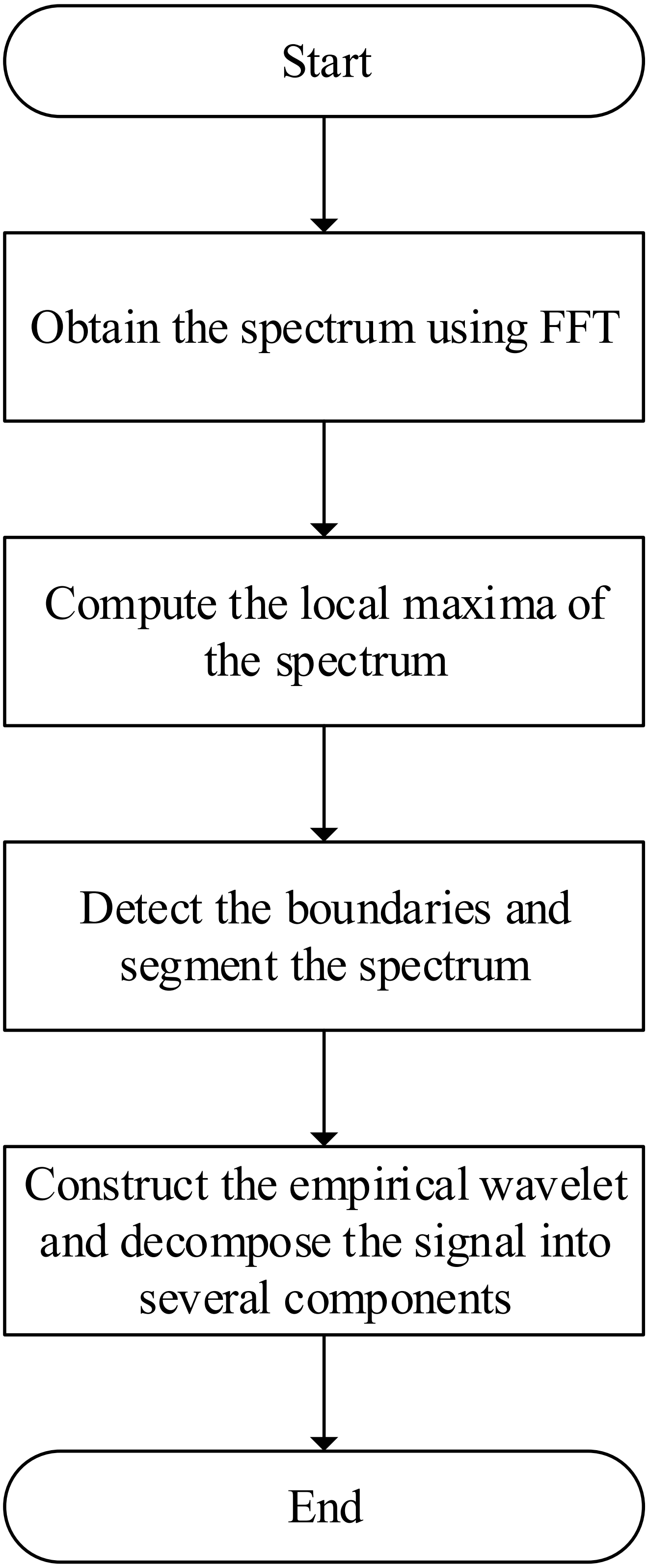

Fig. 1. Flowchart of the EWT method [63].

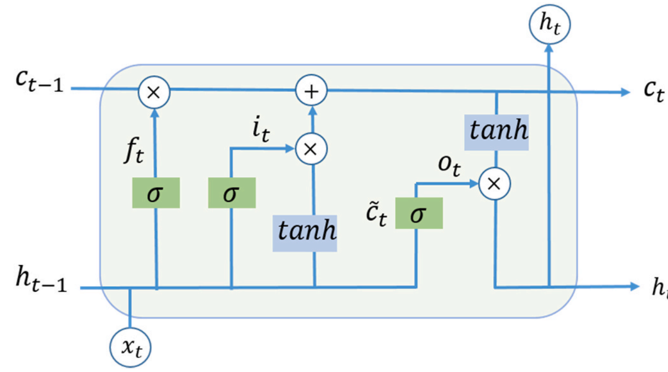

Fig. 2. The configuration of LSTM cell.

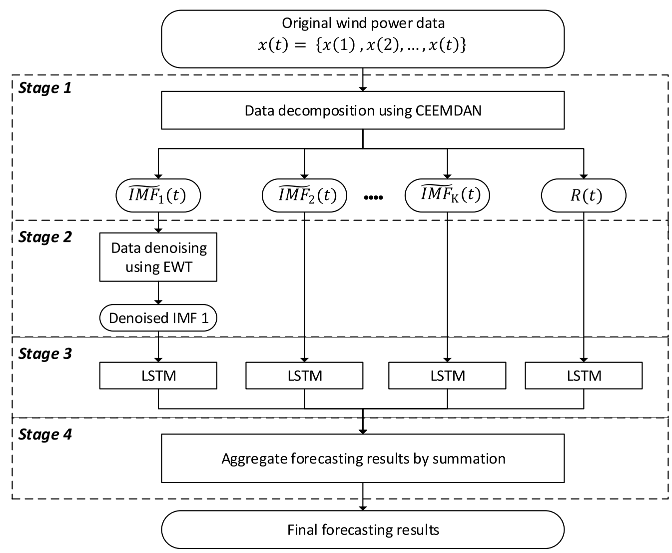

Fig. 3. The general framework of the proposed method.

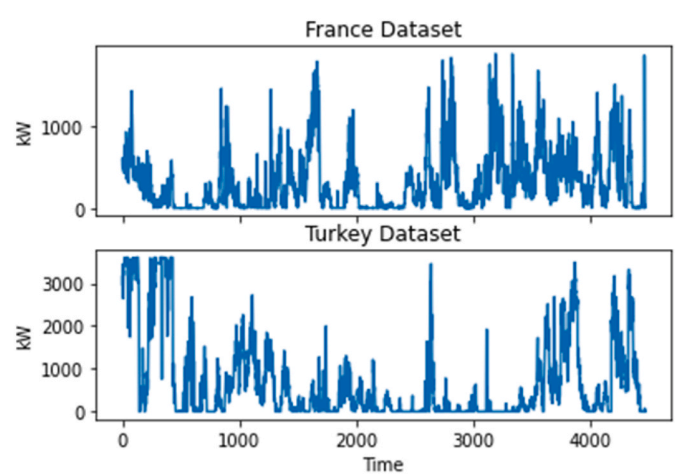

Fig. 4. Wind power data from France and Turkey Dataset in July.

top of the Empirical Mode Decomposition algorithm [52]. EMD was first proposed by Huang et al. [53] and it has the problem of mode mixing, which led to the development of Ensemble Empirical Mode Decomposition (EEMD) to address this issue [54]. Despite its effectiveness, EEMD has some limitations, such as high computational costs [55]. To overcome this limitation, the CEEMDAN algorithm is proposed to enhance the EEMD algorithm by adding adaptive noise into the residual signal after EMD decomposition, rather than adding the noise directly to the original signal [56]. The primary difference between CEEMDAN and EEMD is their approach to adding white-noise components. EEMD decomposes each signal realization with noise into modes independently,

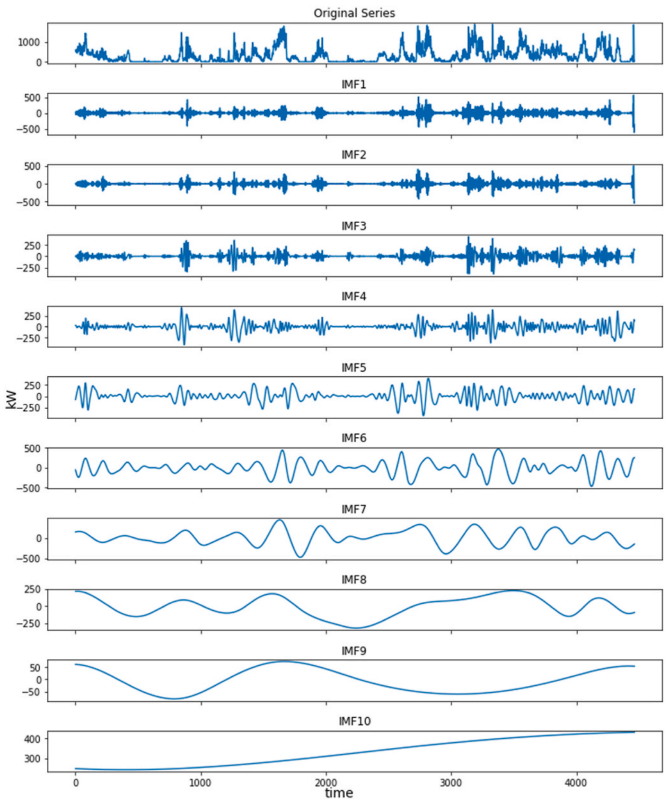

Fig. 5. Decomposition results for the France dataset in July.

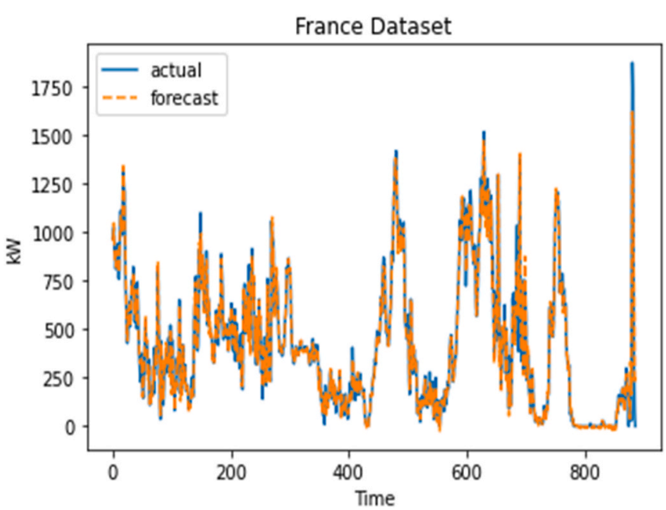

Fig. 6. Comparison between the observed and forecast values for France dataset in July.

with the residuals obtained from each realization not dependent on each other. In contrast, CEEMDAN adds noise to the residual obtained from the previous iteration rather than the original noise. CEEMDAN uses the noise's mode corresponding to the iteration obtained with EMD instead of the noise itself. This approach results in adaptive noise averaged at each iteration and does not introduce additional input to the original signal [57]. CEEMDAN is a significant improvement over EEMD and it has lower computational cost and better decomposition results [58]. The detailed decomposition steps of the CEEMDAN algorithm are as follows [59]:

Let $x(t) = \{x(1), x(2) \ldots, x(t)\}$ represent the original time series data

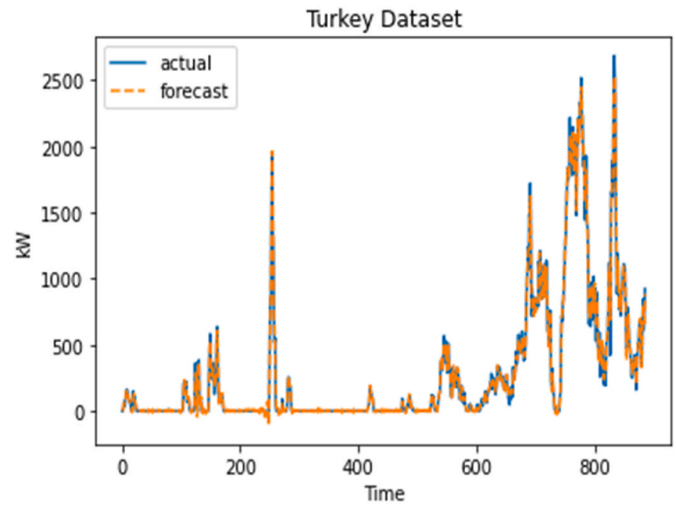

Fig. 7. Comparison between the observed and forecast values for Turkey dataset in July.

and $\widetilde{IMF}_k(t) = \{\widetilde{IMF}_k(1), \widetilde{IMF}_k(t), \ldots, \widetilde{IMF}_k(t)\}$ be k th IMF obtained by the CEEMDAN method. $E_k(\cdot)$ represent the kth IMF generated by the EMD decomposition method. The scalar coefficient ϵ_k is used to set each stage's signal-to-noise ratio (SNR), which determines the standard deviation of the added white noise.

Step 1. Add different realizations of the white noise series $w^i(t)(i = 1, 2, 3, \ldots, L) = \left\{ \begin{bmatrix} w^1(1) & \cdots & w^L(1) \\ \vdots & \ddots & \vdots \\ w^1(t) & \cdots & w^L(t) \end{bmatrix} \right\}$ with an (SNR) of ϵ_0 to the original time series data $x(t)$, where t represents a different time point, i represents the i th white noise added, and L is the total number of times adding white noise. A new time series is constructed as follows:

$$x^i(t) = x(t) + \epsilon_0 w^i(t), i = 1, 2, 3, \ldots, L \tag{1}$$

Step 2. The first IMFs are obtained by EMD shifting procedures [53] and then compute the mean of the component as:

$$\widetilde{IMF}_1(t) = \frac{1}{I} \sum_{i=1}^{L} IMF_1^i(t) = \overline{IMF}_1(t) \tag{2}$$

Step 3. Compute the first residue as:

$$r_1(t) = x(t) - \widetilde{IMF}_1(t) \tag{3}$$

Step 4. To achieve the second mode $\widetilde{IMF}_2(t)$, the $r_1(t) + \varepsilon_1 E_1(w^i(t))$, $i = 1, \ldots, I$ is further decomposed until their first EMD mode is obtained and then compute:

$$\widetilde{IMF}_2(t) = \frac{1}{I} \sum\nolimits_{i=1}^{I} E_1\left(r_1(t) + \varepsilon_1 E_1\left(w^i(t)\right)\right) \tag{4}$$

Step 5. Compute the k - th residue for $= 2, \ldots, K$:

$$r_k(t) = r_{(k-1)}(t) - \widetilde{IMF}_k(t) \tag{5}$$

Step 6. Decompose realizations $r_k(t) + \varepsilon_k E_k(w^i(t)), i = 1, \ldots, I$ until their first EMD mode is obtained and then compute the (k +1)-th mode as:

Table 1
Performance Accuracy of different forecasting methods in the France Dataset.

Month	Metrics	Forecasting Methods							
		SVR	ANN	RF	LSTM	EMD LSTM	EEMD LSTM	CEEMDAN LSTM	Proposed Method
Jan	MAPE	5.46	3.72	4.41	3.44	1.66	1.68	1.58	**1.19**
	RMSE	165.74	112.39	122.09	106.85	53.00	53.22	58.54	**35.12**
	MAE	111.95	76.30	90.36	70.50	33.96	34.48	32.35	**24.36**
Feb	MAPE	8.92	6.08	8.54	5.87	3.02	2.90	2.84	**2.54**
	RMSE	232.90	179.06	216.59	169.86	98.89	91.40	94.51	**76.19**
	MAE	183.00	124.58	175.16	120.35	61.91	59.47	58.15	**52.14**
Mar	MAPE	3.26	3.16	3.19	2.84	1.25	1.35	1.16	**1.03**
	RMSE	119.93	98.79	105.40	89.87	38.58	43.23	38.72	**34.90**
	MAE	66.93	64.73	65.35	58.21	25.58	27.66	23.78	**21.13**
Apr	MAPE	2.98	3.01	2.97	2.96	1.83	1.49	1.53	**1.13**
	RMSE	118.17	111.57	112.85	115.68	62.55	51.99	61.69	**41.24**
	MAE	61.06	61.69	60.93	60.66	37.45	30.47	31.28	**23.17**
May	MAPE	3.69	3.38	3.81	3.20	1.88	1.73	1.82	**1.21**
	RMSE	106.82	104.98	111.25	103.98	67.35	61.98	65.54	**38.57**
	MAE	75.73	69.22	78.11	65.67	38.61	35.57	37.40	**24.76**
Jun	MAPE	6.49	5.13	6.18	4.90	2.92	2.73	2.76	**2.16**
	RMSE	180.15	165.79	172.94	160.27	109.33	98.41	103.01	**70.94**
	MAE	133.11	105.27	126.76	100.47	59.90	55.90	56.65	**44.37**
Jul	MAPE	5.72	4.59	5.41	4.40	2.17	2.31	2.26	**1.88**
	RMSE	164.08	142.84	151.88	137.11	68.91	89.03	91.22	**60.03**
	MAE	117.30	94.07	111.04	90.23	44.59	47.47	46.29	**38.62**
Aug	MAPE	2.48	2.53	2.47	2.31	1.17	1.23	1.09	**0.92**
	RMSE	90.13	90.75	90.62	87.00	45.25	46.19	47.18	**35.10**
	MAE	50.85	51.88	50.64	47.38	23.93	25.20	22.39	**18.86**
Sep	MAPE	1.47	1.65	1.48	1.35	0.90	0.87	0.66	**0.57**
	RMSE	71.90	70.36	68.90	62.88	37.24	30.80	27.95	**23.80**
	MAE	30.18	33.85	30.41	27.73	18.48	17.87	13.52	**11.59**
Oct	MAPE	3.27	3.41	3.33	3.08	2.24	1.58	1.40	**1.20**
	RMSE	102.03	103.86	108.91	100.84	72.91	50.67	50.79	**40.58**
	MAE	67.03	69.90	68.29	63.26	45.90	32.43	28.65	**24.64**
Nov	MAPE	3.88	3.88	4.23	3.83	1.90	1.74	1.54	**1.47**
	RMSE	113.71	114.06	124.93	112.41	57.06	54.32	50.35	**44.07**
	MAE	79.67	79.51	86.68	78.64	38.87	35.62	31.51	**30.04**
Dec	MAPE	9.97	6.01	8.37	6.93	3.10	2.82	2.69	**2.20**
	RMSE	306.32	168.39	230.08	196.20	92.61	83.19	82.43	**64.74**
	MAE	204.36	123.33	171.57	142.13	63.60	57.90	55.21	**45.19**
	MAPE	4.80	3.88	4.53	3.76	2.00	1.87	1.78	**1.46**
Average	RMSE	147.66	121.90	134.70	120.25	66.97	62.87	64.33	**47.11**
	MAE	98.43	79.53	92.94	77.10	41.07	38.34	36.43	**29.91**

$$\widetilde{IMF}_{(k+1)}(t) = \frac{1}{I}\sum\nolimits_{i=1}^{I} E_1\left(r_k(t) + \varepsilon_k E_k\left(w^i(t)\right)\right) \tag{6}$$

Step 7. Go to step 5 for the next k.

In order to acquire the IMF components, the processes in step 5 through step 7 are performed until the residual becomes monotonic and EMD cannot further decompose it. A total of K IMFs are obtained from the CEEMDAN method. As a result, the original data can be decomposed and are expressed as follows:

$$x(t) = \sum\nolimits_{k=1}^{K} \widetilde{IMF}_k(t) + R(t) \tag{7}$$

2.2. Empirical Wavelet Transform (EWT)

Empirical wavelet transform is an adaptive signal processing technique that constructs empirical scaling and wavelet functions based on the frequency spectrum of the signal [60]. The basic idea behind EWT is to calculate the Fourier segment and then construct a series of wavelet filters to extract different modes from the given signal [61]. The overview of the EWT method can be summarized in the following steps [47]:

1. First, apply the FFT to the original signal $x(t)$ to derive its frequency spectrum $x_{(\omega)}$. Identify the maxima in the spectrum $x_{(\omega)}$ and their corresponding frequencies. Suppose the spectrum contains P maxima with frequencies $\omega_i, i = 1, 2, \ldots P$. Sort the maxima in decreasing order according to their magnitude.
2. The next step involves segmenting the Fourier spectrum. To divide the spectrum $(0, \pi)$ into $N (N \leq P)$ sections, the first $(N-1)$ maxima are selected while excluding 0 and π. The boundary of Ω_i for each segment is defined as the midpoint between two consecutive maxima.

$$\Omega_i = \frac{\omega_i + \omega_{i+1}}{2} \tag{8}$$

This yields a set of boundaries $\Omega = \{\Omega_i\}, i = 1, 2, \ldots, N-1$.

3. Build an adaptive wavelet filter bank that incorporates a low-pass filter (scaling function) $\widehat{\varphi}_n(\omega)$ and $(N-1)$ bandpass filter (wavelet functions) $\widehat{\psi}_n(\omega)$ using the identified boundaries [62].

$$\widehat{\varphi}_n(\omega) = \begin{cases} 1 \ \text{if}\ |\omega| \leq (1-\gamma)\omega_n \\ \cos\left[\frac{\pi}{2}\beta\left(\frac{1}{2\gamma\omega_n}(|\omega| - (1-\gamma)\omega_n)\right)\right] \ \text{if}\ (1-\gamma)\omega_n \leq |\omega| \leq (1+\gamma)\omega_n \\ 0 \ otherwise \end{cases} \tag{9}$$

Table 2
Performance Accuracy of different forecasting methods in the Turkey Dataset.

Month	Metrics	Forecasting Methods							
		SVR	ANN	RF	LSTM	EMD LSTM	EEMD LSTM	CEEMDAN LSTM	Proposed Method
Jan	MAPE	5.05	3.18	4.31	2.61	5.64	1.76	1.65	**1.41**
	RMSE	533.82	281.36	395.40	269.38	370.98	145.18	167.75	**121.68**
	MAE	182.66	115.16	155.96	94.57	203.93	63.73	59.85	**50.90**
Feb	MAPE	7.04	4.65	6.83	3.62	2.42	2.10	2.19	**1.64**
	RMSE	480.75	309.29	410.40	266.11	150.48	137.91	140.58	**102.72**
	MAE	254.80	168.44	247.07	131.10	87.48	76.10	79.12	**59.44**
Mar	MAPE	6.28	4.75	6.70	4.54	2.51	2.55	2.23	**1.83**
	RMSE	335.30	304.62	354.01	287.65	167.25	156.50	147.69	**115.76**
	MAE	227.22	171.77	242.38	164.13	90.82	92.20	80.65	**66.33**
Apr	MAPE	4.29	3.12	4.87	2.71	1.56	1.41	1.19	**1.09**
	RMSE	206.86	189.64	228.97	171.71	94.01	81.74	72.49	**65.31**
	MAE	155.42	112.89	176.25	98.11	56.56	51.03	43.18	**39.42**
May	MAPE	9.71	6.32	8.66	6.24	3.11	2.84	2.72	**2.29**
	RMSE	473.05	322.12	406.70	318.82	164.97	161.55	156.07	**122.68**
	MAE	351.44	228.72	313.50	225.73	112.53	102.82	98.25	**82.80**
Jun	MAPE	10.17	7.12	9.18	6.87	3.17	3.10	3.27	**2.60**
	RMSE	520.86	381.57	434.38	354.32	159.36	158.45	187.77	**130.95**
	MAE	368.08	257.75	332.25	248.49	114.89	112.17	118.35	**93.96**
Jul	MAPE	1.81	1.81	1.78	1.85	1.17	0.99	0.83	**0.66**
	RMSE	140.61	131.74	134.84	127.04	71.18	57.95	58.57	**45.57**
	MAE	65.37	65.35	64.30	66.77	42.39	35.96	29.97	**24.00**
Aug	MAPE	6.71	4.31	6.41	3.87	2.21	1.80	1.56	**1.45**
	RMSE	420.21	225.34	341.90	209.83	111.19	105.23	92.73	**78.01**
	MAE	242.93	155.81	231.95	139.90	79.99	64.97	56.43	**52.60**
Sep	MAPE	10.23	4.72	8.58	4.45	2.43	1.98	1.66	**1.51**
	RMSE	637.89	249.90	469.70	241.14	146.52	110.71	99.24	**86.88**
	MAE	370.06	170.93	310.51	161.19	87.87	71.50	60.20	**54.58**
Oct	MAPE	3.81	4.22	3.98	3.49	2.44	1.76	1.51	**1.15**
	RMSE	204.47	235.81	215.02	200.51	123.42	93.83	88.45	**62.26**
	MAE	137.70	152.71	143.93	126.46	88.27	63.74	54.59	**41.46**
Nov	MAPE	10.03	2.50	6.03	2.18	1.48	1.47	1.25	**1.04**
	RMSE	944.06	226.74	475.99	212.76	105.67	108.54	99.66	**81.22**
	MAE	362.78	90.39	218.15	78.95	53.54	53.37	45.10	**37.64**
Dec	MAPE	2.16	1.22	2.74	1.03	1.00	0.88	0.57	**0.45**
	RMSE	342.58	125.07	286.66	120.84	81.45	56.91	46.03	**39.64**
	MAE	78.22	44.05	99.28	37.17	36.03	31.95	20.68	**16.14**
Average	MAPE	6.44	3.99	5.84	3.62	2.43	1.89	1.72	**1.43**
	RMSE	436.70	248.60	346.16	231.68	145.54	114.54	113.09	**87.72**
	MAE	233.06	144.50	211.29	131.05	87.86	68.30	62.20	**51.61**

$$\widehat{\psi}_n(\omega) = \begin{cases} 1 \quad \text{if } (1+\gamma)\omega_n \le |\omega| \le (1-\gamma)\omega_{n+1} \\ \cos\left[\frac{\pi}{2}\beta\left(\frac{1}{2\gamma\omega_{n+1}}(|\omega| - (1-\gamma)\omega_{n+1})\right)\right] \quad \text{if } (1-\gamma)\omega_{n+1} \le |\omega| \le (1+\gamma)\omega_{n+1} \\ \sin\left[\frac{\pi}{2}\beta\left(\frac{1}{2\gamma\omega_n}(|\omega| - (1-\gamma)\omega_n)\right)\right] \quad \text{if } (1-\gamma)\omega_n \le |\omega| \le (1+\gamma)\omega_n \\ \textit{otherwise} \end{cases} \tag{10}$$

$$\beta(x) = \begin{cases} 0 \quad \textit{if} \text{ if } x \le 0 \\ \text{and } \beta(x) + \beta(1-x) = 1 \forall x \in [0,1] \\ 1 \quad \text{if } x \ge 1 \end{cases} \tag{11}$$

4. At last, the extracted modes are established as the output of the scaling function and wavelet functions.

The flowchart of the EWT method is described in Fig. 1 [63].

2.3. Long Short-Term Memory (LSTM)

Long Short-Term Memory (LSTM) is a prominent deep learning method for time series forecasting [64]. It has an excellent memory capability and it can find regular information from wind power historical data [65]. LSTM introduces the “gates” mechanism to enhance the basic functionalities of recurrent cell memory [66]. This gate mechanism enables LSTM to control the flow of information [67]. Thus, LSTM is able to preserve important information for a longer period and ignore less useful historical information from time series data. Due to its special architecture, LSTM is suitable for ultra-short-term wind forecasting [68]. Fig. 2 illustrates the structure of the LSTM cell which is comprised

Table 3
Percentage improvement of Proposed Method vs. Other Benchmarking Methods in France Dataset.

Month	Improvement Percentage Metrics	Proposed Method vs SVR	Proposed Method vs ANN	Proposed Method vs RF	Proposed Method vs LSTM	Proposed Method vs EMD LSTM	Proposed Method vs EEMD LSTM	Proposed Method vs CEEMDAN LSTM
Jan	P_{MAPE}	78.24%	68.08%	73.04%	65.45%	28.28%	29.35%	24.71%
	P_{RMSE}	78.81%	68.75%	71.23%	67.13%	33.74%	34.01%	40.00%
	P_{MAE}	78.24%	68.08%	73.04%	65.45%	28.28%	29.35%	24.71%
Feb	P_{MAPE}	71.51%	58.15%	70.23%	56.67%	15.78%	12.32%	10.32%
	P_{RMSE}	67.29%	57.45%	64.82%	55.15%	22.96%	16.65%	19.39%
	P_{MAE}	71.51%	58.15%	70.23%	56.67%	15.78%	12.32%	10.32%
Mar	P_{MAPE}	68.44%	67.36%	67.67%	63.71%	17.41%	23.62%	11.17%
	P_{RMSE}	70.90%	64.67%	66.89%	61.16%	9.53%	19.27%	9.86%
	P_{MAE}	68.44%	67.36%	67.67%	63.71%	17.41%	23.62%	11.17%
Apr	P_{MAPE}	62.06%	62.44%	61.98%	61.81%	38.14%	23.97%	25.95%
	P_{RMSE}	65.10%	63.04%	63.46%	64.35%	34.07%	20.67%	33.15%
	P_{MAE}	62.06%	62.44%	61.98%	61.81%	38.14%	23.97%	25.95%
May	P_{MAPE}	67.30%	64.22%	68.30%	62.29%	35.86%	30.39%	33.79%
	P_{RMSE}	63.89%	63.25%	65.33%	62.90%	42.72%	37.76%	41.14%
	P_{MAE}	67.30%	64.22%	68.30%	62.29%	35.86%	30.39%	33.79%
Jun	P_{MAPE}	66.67%	57.85%	65.00%	55.84%	25.93%	20.63%	21.69%
	P_{RMSE}	60.62%	57.21%	58.98%	55.74%	35.12%	27.91%	31.13%
	P_{MAE}	66.67%	57.85%	65.00%	55.84%	25.93%	20.63%	21.69%
Jul	P_{MAPE}	67.08%	58.95%	65.22%	57.20%	13.38%	18.64%	16.57%
	P_{RMSE}	63.41%	57.97%	60.47%	56.21%	12.88%	32.57%	34.19%
	P_{MAE}	67.08%	58.95%	65.22%	57.20%	13.38%	18.64%	16.57%
Aug	P_{MAPE}	62.91%	63.65%	62.75%	60.19%	21.20%	25.16%	15.76%
	P_{RMSE}	61.06%	61.33%	61.27%	59.66%	22.43%	24.01%	25.62%
	P_{MAE}	62.91%	63.65%	62.75%	60.19%	21.20%	25.16%	15.76%
Sep	P_{MAPE}	61.59%	65.75%	61.88%	58.19%	37.27%	35.13%	14.28%
	P_{RMSE}	66.89%	66.17%	65.45%	62.14%	36.08%	22.72%	14.83%
	P_{MAE}	61.59%	65.75%	61.88%	58.19%	37.27%	35.13%	14.28%
Oct	P_{MAPE}	63.24%	64.75%	63.92%	61.05%	46.32%	24.02%	13.99%
	P_{RMSE}	60.23%	60.93%	62.74%	59.76%	44.34%	19.91%	20.11%
	P_{MAE}	63.24%	64.75%	63.92%	61.05%	46.32%	24.02%	13.99%
Nov	P_{MAPE}	62.29%	62.21%	65.34%	61.80%	22.71%	15.67%	4.67%
	P_{RMSE}	61.25%	61.37%	64.73%	60.80%	22.77%	18.87%	12.49%
	P_{MAE}	62.29%	62.21%	65.34%	61.80%	22.71%	15.67%	4.67%
Dec	P_{MAPE}	77.89%	63.35%	73.66%	68.20%	28.95%	21.94%	18.14%
	P_{RMSE}	78.87%	61.56%	71.86%	67.01%	30.10%	22.18%	21.46%
	P_{MAE}	77.89%	63.35%	73.66%	68.20%	28.95%	21.94%	18.14%
Average	P_{MAPE}	67.41%	62.75%	66.48%	60.74%	26.51%	23.04%	17.51%
	P_{RMSE}	66.29%	61.67%	64.44%	60.63%	27.66%	25.32%	25.97%
	P_{MAE}	67.41%	62.75%	66.48%	60.74%	26.51%	23.04%	17.51%

of an input gate, output gate, and forget gate [69].

The equations for the LSTM model are as follows [70]:

$$f_t = \sigma\left(W_f \cdot [h_{t-1}, x_t] + b_f\right) \tag{12}$$

$$i_t = \sigma(W_i \cdot [h_{t-1}, x_t] + b_i) \tag{13}$$

$$o_t = \sigma(W_o \cdot [h_{t-1}, x_t] + b_o) \tag{14}$$

$$\widetilde{c}_t = tanh(W_C \cdot [h_{t-1}, x_t] + b_C) \tag{15}$$

$$c_t = f_t \otimes c_{t-1} + i_t \otimes \widetilde{c}_t \tag{16}$$

$$h_t = o_t \otimes \tanh(c_t) \tag{17}$$

where W_f, W_t, W_c , W_σ are the set of weights, b_f, b_i, b_c, b_o are the corresponding bias vectors and $\otimes$ is element-wise multiplication. σ is the sigmoid function $\sigma = \frac{1}{1+e^{-z}}$ and tanh is the tanh function $\frac{e^x-e^{-x}}{e^x+e^{-x}}$. f_t is the forget gate, i_t is the input gate, o_t is the output gate, c_t is the cell-state vector at time-step t, h_t represents the output of the LSTM at time t and x_t is the input. Forget gate determines what information should be removed and the input gate decides what information should be kept.

3. The framework of the proposed method

In this study, a hybrid approach using CEEMDAN EWT-LSTM for ultra-short-term wind power forecasting was introduced. The general framework of the proposed method is depicted Fig. 3.

The detailed procedures of the proposed method are as follows:

- **Stage 1:** In the proposed method, the original wind data is first preprocessed using the CEEMDAN decomposition technique into several subseries named Intrinsic Mode Functions (IMFs). CEEMDAN was employed in this study since this approach produces better decomposition results and is more computationally efficient compared to EEMD and CEEMD [71].
- **Stage 2:** The first IMF series generated by CEEMDAN in the first stage is the most irregular series, which may deteriorate the forecasting accuracy. To handle the first IMF series, the EWT denoising technique is applied to denoise the first IMF. At this stage, the original IMF 1 data will be preprocessed using EWT and several meaningful empirical modes will be acquired, as well as the residual. Then, the residual is eliminated since it mainly consists of noisy signals [51], and the remaining modes are aggregated to form a new denoised series of IMF 1. By denoising IMF 1, the negative impact of randomness and irregularities on IMF 1 can be reduced, which makes IMF 1 more suitable for forecasting and can easily be modeled.
- **Stage 3:** The LSTM forecasting method is utilized to forecast all subseries obtained by the CEEMDAN-EWT.
- **Stage 4:** All the forecasting results for each subseries are added together to obtain the final forecasting results.

Table 4
Percentage improvement of Proposed Method vs. Other Benchmarking Methods in Turkey Dataset.

Month	Improvement Percentage Metrics	Proposed Method vs SVR	Proposed Method vs ANN	Proposed Method vs RF	Proposed Method vs LSTM	Proposed Method vs EMD LSTM	Proposed Method vs EEMD LSTM	Proposed Method vs CEEMDAN LSTM
Jan	P_{MAPE}	72.14%	55.80%	67.36%	46.18%	75.04%	20.13%	14.96%
	P_{RMSE}	77.21%	56.75%	69.23%	54.83%	67.20%	16.19%	27.46%
	P_{MAE}	72.14%	55.80%	67.36%	46.18%	75.04%	20.13%	14.96%
Feb	P_{MAPE}	76.67%	64.71%	75.94%	54.66%	32.05%	21.90%	24.87%
	P_{RMSE}	78.63%	66.79%	74.97%	61.40%	31.74%	25.52%	26.93%
	P_{MAE}	76.67%	64.71%	75.94%	54.66%	32.05%	21.90%	24.87%
Mar	P_{MAPE}	70.81%	61.38%	72.63%	59.59%	26.96%	28.06%	17.76%
	P_{RMSE}	65.48%	62.00%	67.30%	59.76%	30.79%	26.03%	21.62%
	P_{MAE}	70.81%	61.38%	72.63%	59.59%	26.96%	28.06%	17.76%
Apr	P_{MAPE}	74.64%	65.08%	77.63%	59.82%	30.30%	22.75%	8.70%
	P_{RMSE}	68.43%	65.56%	71.48%	61.97%	30.53%	20.11%	9.91%
	P_{MAE}	74.64%	65.08%	77.63%	59.82%	30.30%	22.75%	8.70%
May	P_{MAPE}	76.44%	63.80%	73.59%	63.32%	26.42%	19.47%	15.73%
	P_{RMSE}	74.07%	61.92%	69.84%	61.52%	25.64%	24.07%	21.40%
	P_{MAE}	76.44%	63.80%	73.59%	63.32%	26.42%	19.47%	15.73%
Jun	P_{MAPE}	74.47%	63.55%	71.72%	62.19%	18.22%	16.23%	20.61%
	P_{RMSE}	74.86%	65.68%	69.85%	63.04%	17.83%	17.36%	30.26%
	P_{MAE}	74.47%	63.55%	71.72%	62.19%	18.22%	16.23%	20.61%
Jul	P_{MAPE}	63.28%	63.27%	62.67%	64.05%	43.37%	33.26%	19.91%
	P_{RMSE}	67.59%	65.41%	66.21%	64.13%	35.98%	21.37%	22.20%
	P_{MAE}	63.28%	63.27%	62.67%	64.05%	43.37%	33.26%	19.91%
Aug	P_{MAPE}	78.35%	66.24%	77.32%	62.40%	34.24%	19.04%	6.78%
	P_{RMSE}	81.43%	65.38%	77.18%	62.82%	29.84%	25.86%	15.87%
	P_{MAE}	78.35%	66.24%	77.32%	62.40%	34.24%	19.04%	6.78%
Sep	P_{MAPE}	85.25%	68.07%	82.42%	66.14%	37.89%	23.66%	9.34%
	P_{RMSE}	86.38%	65.23%	81.50%	63.97%	40.71%	21.53%	12.46%
	P_{MAE}	85.25%	68.07%	82.42%	66.14%	37.89%	23.66%	9.34%
Oct	P_{MAPE}	69.89%	72.85%	71.19%	67.21%	53.03%	34.95%	24.04%
	P_{RMSE}	69.55%	73.60%	71.05%	68.95%	49.56%	33.65%	29.62%
	P_{MAE}	69.89%	72.85%	71.19%	67.21%	53.03%	34.95%	24.04%
Nov	P_{MAPE}	89.63%	58.36%	82.75%	52.33%	29.71%	29.48%	16.55%
	P_{RMSE}	91.40%	64.18%	82.94%	61.83%	23.13%	25.17%	18.50%
	P_{MAE}	89.63%	58.36%	82.75%	52.33%	29.71%	29.48%	16.55%
Dec	P_{MAPE}	79.37%	63.37%	83.75%	56.59%	55.21%	49.49%	21.97%
	P_{RMSE}	88.43%	68.31%	86.17%	67.20%	51.33%	30.35%	13.88%
	P_{MAE}	79.37%	63.37%	83.75%	56.59%	55.21%	49.49%	21.97%
Average	P_{MAPE}	74.94%	63.83%	73.97%	59.89%	38.91%	27.05%	17.01%
	P_{RMSE}	76.23%	65.09%	73.38%	62.73%	36.17%	23.73%	20.95%
	P_{MAE}	74.94%	63.83%	73.97%	59.89%	38.91%	27.05%	17.01%

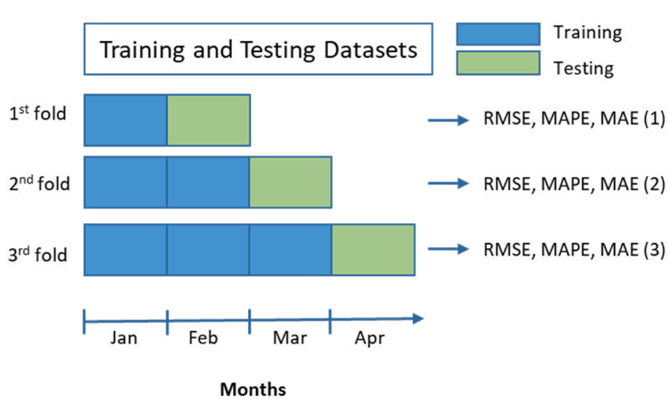

Fig. 8. A visual representation of the time series cross-validation framework.

4. Experimental results

4.1. Dataset

The performance of the proposed method is tested by using wind power datasets in two different countries. The first dataset is from a wind farm with an installed capacity of 2050 kW located in France,[1] and the second dataset is from a wind farm with an installed capacity of 3600 kW located in Turkey.[2] In this study, data from two datasets with 10-min intervals over a one-year period was utilized. The first 80% of the data was utilized as a training data set and the remaining was utilized as a testing dataset. The model was developed using the training data set and the forecasting performance was evaluated using the testing dataset. Fig. 4 depicts plots of wind power observations from the France and Turkey datasets in July. As can be seen from Fig. 4, wind power data presents nonstationary and nonlinear characteristics, which makes it difficult to establish accurate wind power forecasts.

4.2. Experimental settings

In this study, the experiments were implemented in Python 3.7 on a PC with Intel Core i3-8130U CPU, 2.20 GHz, with a memory size of 4.00 GB. The pyEMD package in python was utilized to implement CEEMDAN [46] and the ewtpy package [47] for implementing EWT. Keras [48] was used as a tool for implementing the LSTM. For LSTM configuration, Adam was used as the optimizer as it has proven to be effective compared to other stochastic optimization methods [49,50]. As suggested in Ref. [51], the learning rate of LSTM is set as 0.001 and the method was trained for 100 epochs [52].

1 https://opendata-renewables.engie.com/explore/?sort=modified.
2 https://www.kaggle.com/datasets/berkerisen/wind-turbine-scada-dataset.

Table 5
Time-series cross-validation results for the France and Turkey Dataset.

Dataset	Fold	Metrics	Forecasting Methods							
			SVR	ANN	RF	LSTM	EMD LSTM	EEMD LSTM	CEEMDAN LSTM	Proposed Method
France	1	MAPE	4.86	4.06	4.74	3.93	1.94	1.88	1.78	**1.51**
		RMSE	137.59	134.51	140.36	130.29	67.47	63.98	66.07	**53.82**
		MAE	99.76	83.17	97.13	80.50	39.86	38.64	36.46	**30.87**
	2	MAPE	4.13	4.05	4.69	3.93	1.75	1.82	1.62	**1.48**
		RMSE	126.01	127.59	136.14	125.26	57.94	62.13	59.81	**49.06**
		MAE	84.60	83.11	96.13	80.64	35.92	37.37	33.18	**30.30**
	3	MAPE	2.95	2.77	2.86	2.74	1.31	1.29	1.08	**1.02**
		RMSE	105.72	91.67	100.00	93.60	46.69	44.16	42.00	**38.20**
		MAE	60.56	56.78	58.65	56.20	26.94	26.42	22.22	**20.93**
	Average	MAPE	3.98	3.63	4.09	3.53	1.67	1.66	1.49	**1.33**
		RMSE	123.11	117.92	125.50	116.38	57.37	56.76	55.96	**47.03**
		MAE	81.64	74.35	83.97	72.45	34.24	34.14	30.62	**27.36**
Turkey	1	MAPE	5.01	4.71	5.36	3.74	2.34	1.93	1.71	**1.37**
		RMSE	269.32	275.47	293.93	245.93	170.54	132.27	121.98	**90.90**
		MAE	181.23	170.48	193.93	135.26	84.72	70.00	62.04	**49.75**
	2	MAPE	7.23	4.75	7.95	4.57	2.49	2.25	2.01	**1.83**
		RMSE	391.79	314.55	402.76	317.37	165.97	157.17	151.48	**121.87**
		MAE	261.50	172.00	287.63	165.51	89.95	81.43	72.67	**66.32**
	3	MAPE	7.07	3.26	6.51	3.54	1.47	1.39	1.15	**1.01**
		RMSE	555.92	229.51	430.84	273.29	125.84	105.65	103.61	**83.53**
		MAE	255.72	118.10	235.66	128.03	53.03	50.35	41.79	**36.43**
	Average	MAPE	6.43	4.24	6.61	3.95	2.10	1.86	1.63	**1.40**
		RMSE	405.67	273.18	375.84	278.86	154.12	131.70	125.69	**98.77**
		MAE	232.82	153.53	239.07	142.93	75.90	67.26	58.83	**50.83**

Table 6
Percentage improvement in time-series cross-validation of proposed method compared to other benchmarking methods for France and Turkey datasets.

Dataset	Fold	Improvement Percentage Metrics	Proposed Method vs SVR	Proposed Method vs ANN	Proposed Method vs RF	Proposed Method vs LSTM	Proposed Method vs EMD LSTM	Proposed Method vs EEMD LSTM	Proposed Method vs CEEMDAN LSTM
France	1	P_{MAPE}	69.06%	62.89%	68.22%	61.66%	22.57%	20.12%	15.36%
		P_{RMSE}	60.88%	59.98%	61.65%	58.69%	20.22%	15.88%	18.53%
		P_{MAE}	69.06%	62.89%	68.22%	61.66%	22.57%	20.12%	15.36%
	2	P_{MAPE}	64.19%	63.55%	68.48%	62.43%	15.65%	18.93%	8.69%
		P_{RMSE}	61.07%	61.55%	63.96%	60.83%	15.33%	21.04%	17.97%
		P_{MAE}	64.19%	63.55%	68.48%	62.43%	15.65%	18.93%	8.69%
	3	P_{MAPE}	65.44%	63.14%	64.31%	62.76%	22.31%	20.78%	5.80%
		P_{RMSE}	63.87%	58.33%	61.80%	59.19%	18.19%	13.51%	9.05%
		P_{MAE}	65.44%	63.14%	64.31%	62.76%	22.31%	20.78%	5.80%
	Average	P_{MAPE}	66.23%	63.19%	67.01%	62.28%	20.18%	19.94%	9.95%
		P_{RMSE}	61.94%	59.95%	62.47%	59.57%	17.91%	16.81%	15.19%
		P_{MAE}	66.23%	63.19%	67.01%	62.28%	20.18%	19.94%	9.95%
Turkey	1	P_{MAPE}	72.55%	70.82%	74.35%	63.22%	41.28%	28.94%	19.82%
		P_{RMSE}	66.25%	67.00%	69.07%	63.04%	46.70%	31.28%	25.48%
		P_{MAE}	72.55%	70.82%	74.35%	63.22%	41.28%	28.94%	19.82%
	2	P_{MAPE}	74.64%	61.44%	76.94%	59.93%	26.27%	18.56%	8.73%
		P_{RMSE}	68.89%	61.26%	69.74%	61.60%	26.57%	22.46%	19.55%
		P_{MAE}	74.64%	61.44%	76.94%	59.93%	26.27%	18.56%	8.73%
	3	P_{MAPE}	85.75%	69.16%	84.54%	71.55%	31.31%	27.66%	12.82%
		P_{RMSE}	84.97%	63.61%	80.61%	69.44%	33.62%	20.94%	19.38%
		P_{MAE}	85.75%	69.16%	84.54%	71.55%	31.31%	27.66%	12.82%
	Average	P_{MAPE}	77.65%	67.14%	78.61%	64.90%	32.95%	25.05%	13.79%
		P_{RMSE}	73.37%	63.95%	73.14%	64.69%	35.63%	24.89%	21.47%
		P_{MAE}	77.65%	67.14%	78.61%	64.90%	32.95%	25.05%	13.79%

Preliminary experiments were performed to determine the ideal number of hidden neurons and batch size for the proposed method [72, 73]. Various combinations of neurons and batch sizes, including values of 32, 64, and 128, were evaluated. It was observed that the configuration with 128 neurons and a batch size of 64 outperformed other combinations. Thus, it is selected to train the proposed method. This study performs a 10-min-ahead forecast (X_t) and the previous 1-h data (X_{t-1} to X_{t-6}) is used as the input of the forecasting method.

4.3. Evaluation metrics

In this study, three common evaluation metrics were used, which are Root Mean Square Error (RMSE), Mean Absolute Percentage Error (MAPE), and Mean Absolute Error (MAE) [74]. The three metrics are defined as follows [74]:

$$RMSE = \sqrt{\frac{1}{N}\sum_{i=1}^{N}(\hat{y}_i - y_i)^2} \tag{18}$$

$$MAPE = \frac{1}{N}\sum_{i=1}^{N}\left|\frac{y_i^{pre} - y_i}{y_{max}}\right| \tag{19}$$

Table 7
Comparative experiment results for Turkey dataset.

Month	Metrics	Forecasting Methods		
		EMD-ENN	EEMD-BO-LSTM	Proposed Method
Jan	MAPE	3.74	1.89	**1.41**
	RMSE	228.74	152.97	**121.68**
	MAE	135.20	68.32	**50.9**
Feb	MAPE	3.60	2.24	**1.64**
	RMSE	207.67	144.63	**102.72**
	MAE	130.18	81.01	**59.44**
Mar	MAPE	3.08	2.51	**1.83**
	RMSE	182.33	158.07	**115.76**
	MAE	111.36	90.92	**66.33**
Apr	MAPE	1.46	1.40	**1.09**
	RMSE	81.57	83.77	**65.31**
	MAE	52.67	50.63	**39.42**
May	MAPE	2.65	3.19	**2.29**
	RMSE	150.39	169.91	**122.68**
	MAE	95.90	115.35	**82.8**
Jun	MAPE	3.77	3.35	**2.6**
	RMSE	177.52	167.15	**130.95**
	MAE	136.27	121.28	**93.96**
Jul	MAPE	1.35	1.00	**0.66**
	RMSE	70.44	59.98	**45.57**
	MAE	48.74	36.32	**24**
Aug	MAPE	1.68	1.79	**1.45**
	RMSE	84.81	107.26	**78.01**
	MAE	60.76	64.75	**52.6**
Sep	MAPE	1.52	1.98	**1.51**
	RMSE	84.84	111.22	**86.88**
	MAE	55.03	71.50	**54.58**
Oct	MAPE	2.06	1.75	**1.15**
	RMSE	95.41	97.79	**62.26**
	MAE	74.58	63.51	**41.46**
Nov	MAPE	1.68	1.41	**1.04**
	RMSE	135.43	105.65	**81.22**
	MAE	60.92	50.88	**37.64**
Dec	MAPE	3.00	0.86	**0.45**
	RMSE	172.90	54.87	**39.64**
	MAE	108.68	30.98	**16.14**
Average	MAPE	2.46	1.95	**1.43**
	RMSE	139.34	117.77	**87.72**
	MAE	89.19	70.45	**51.61**

Table 8
Percentage improvement of proposed method compared to other state-of-the-art methods for Turkey dataset.

Month	Improvement Percentage Metrics	Proposed Method vs EMD-ENN	Proposed Method vs EEMD-BO-LSTM
Jan	P_{MAPE}	62.26%	25.32%
	P_{RMSE}	46.80%	20.46%
	P_{MAE}	62.35%	25.50%
Feb	P_{MAPE}	54.41%	26.74%
	P_{RMSE}	50.54%	28.98%
	P_{MAE}	54.34%	26.62%
Mar	P_{MAPE}	40.53%	27.16%
	P_{RMSE}	36.51%	26.77%
	P_{MAE}	40.44%	27.04%
Apr	P_{MAPE}	25.12%	22.09%
	P_{RMSE}	19.93%	22.03%
	P_{MAE}	25.16%	22.13%
May	P_{MAPE}	13.59%	28.16%
	P_{RMSE}	18.43%	27.80%
	P_{MAE}	13.66%	28.22%
Jun	P_{MAPE}	30.96%	22.42%
	P_{RMSE}	26.24%	21.66%
	P_{MAE}	31.05%	22.53%
Jul	P_{MAPE}	51.00%	34.24%
	P_{RMSE}	35.30%	24.02%
	P_{MAE}	50.76%	33.92%
Aug	P_{MAPE}	13.64%	18.96%
	P_{RMSE}	8.02%	27.27%
	P_{MAE}	13.43%	18.76%
Sep	P_{MAPE}	0.70%	23.58%
	P_{RMSE}	2.41%	21.89%
	P_{MAE}	0.81%	23.67%
Oct	P_{MAPE}	44.20%	34.47%
	P_{RMSE}	34.75%	36.33%
	P_{MAE}	44.41%	34.72%
Nov	P_{MAPE}	38.23%	26.04%
	P_{RMSE}	40.03%	23.12%
	P_{MAE}	38.22%	26.03%
Dec	P_{MAPE}	85.02%	47.44%
	P_{RMSE}	77.07%	27.75%
	P_{MAE}	85.15%	47.90%
Average	P_{MAPE}	38.30%	28.05%
	P_{RMSE}	33.00%	25.67%
	P_{MAE}	38.31%	28.09%

$$MAE = \frac{1}{N}\sum_{i=1}^{N}|y_i^{pre} - y_i| \tag{20}$$

where y_i is the real wind power value at time i and $\hat{y}_i$ is the forecasted wind power value at time i. N denotes the number of data points and y_{max} is the maximum value of the whole data. The lower the value of the evaluation metrics above, the better the performance of the forecasting method. The percentage of improvement [75] is also applied in this study to evaluate the enhancement of the proposed forecasting method compared to other forecasting methods. The percentage of improvements are calculated as follows [72]:

$$P_{RMSE} = \frac{RMSE_1 - RMSE_2}{RMSE_1} * 100\% \tag{21}$$

$$P_{MAPE} = \frac{MAPE_1 - MAPE_2}{MAPE_1} * 100\% \tag{22}$$

$$P_{MAE} = \frac{MAE_1 - MAE_2}{MAE_1} * 100\% \tag{23}$$

4.4. Results

In the initial phase of our proposed method, CEEMDAN was used to transform the original data into several subseries. As wind data exhibits strong nonlinearity and nonstationary characteristics [76], CEEMDAN is used to decompose the original data into several Intrinsic Mode Functions (IMF) with lower nonlinearity and nonstationary characteristics. IMFs extracted from CEEMDAN for the France dataset are shown in Fig. 5. As can be seen in Fig. 5, the frequency of the first IMF is the highest, and the last series of IMF is the lowest frequency. This last series resembles the trend of the series.

Since IMF 1 is the most disordered and irregular series, this condition may affect the accuracy and stability of the forecasting model. To reduce forecasting difficulties, the EWT denoising technique is applied to denoise the first IMF. The EWT denoising technique is adopted to reduce the randomness and fluctuation of the first IMF. By reducing the randomness and fluctuation of the first IMF, it is easier to model the series and the learning capability of forecasting accuracy could be further enhanced. After the data preprocessing step, LSTM is employed to forecast all the series, and all the series are summed up together to obtain the final forecasting results. Figs. 6 and 7 visualize the result obtained from the proposed method. As can be observed from Figs. 6 and 7, the forecasting lines of the proposed method are close to the actual values line with small deviations, which means the proposed method can forecast accurately.

To evaluate the performance of our proposed CEEMDAN-EWT-LSTM method, seven forecasting methods were used as comparisons, which are: Support Vector Regression (SVR), Artificial Neural Network (ANN), Random Forest (RF), Long Short-Term Memory (LSTM), Empirical Mode Decomposition-Long Short-Term Memory (EMD-LSTM), Ensemble empirical mode decomposition-Long Short-Term Memory (EEMD-LSTM) and Complete Ensemble Empirical Mode Decomposition with Adaptive Noise-Long Short-Term Memory (CEEMDAN-LSTM). The first to fourth methods are the single forecasting methods, which are SVR, ANN, RF, and LSTM. The fifth to seventh methods (EMD-LSTM, EEMD-LSTM, and CEEMDAN-LSTM) are hybrid decomposition methods that combine a single data preprocessing technique to decompose the original data and LSTM to forecast all the decomposed subseries separately. The comparison between different forecasting methods for the France dataset and Turkey dataset are presented in Table 1 and Table 2, respectively. To show the forecasting ability of the proposed method more intuitively, the improvement percentages from other benchmarking methods are calculated, and the results are shown in Table 3 and Table 4.

In Tables 1 and 2, the bold values represent the forecasting method with the lowest error in the corresponding dataset, and the values in the last row represent the average values of each evaluation metric. According to the given results, it can be observed that:

1. LSTM can achieve better performance accuracy compared to other single forecasting methods (SVR, ANN, and RF). As shown in Tables 1 and 2, the MAPE, RMSE, and MAE of the LSTM method are the smallest among the single forecasting methods in both datasets. Therefore, it is beneficial to choose LSTM as the base forecasting technique to forecast each subseries in our proposed method.
2. Compared to the single forecasting methods, the hybrid decomposition methods can effectively improve the performance of wind power forecasting. Taking the France dataset as an example, the average MAPE values of the hybrid decomposition methods (EMD-LSTM, EEMD-LSTM, CEEMDAN-LSTM, and proposed CEEMDAN-EWT-LSTM) are 1.46%–2%, which are lower than those of the single forecasting methods (SVR, ANN, RF, and LSTM). Since original wind data exhibits high volatility and nonstationary characteristics, it has been difficult to forecast wind data with a single method. By decomposing the original wind data into several more relatively stationary subseries, the quality of the input data of the forecasting model could be enhanced and each subseries could be forecasted more effectively. Therefore, the hybrid decomposition methods perform better than the single forecasting methods.
3. Using different data decomposition approaches, CEEMDAN shows superiority over EMD and EEMD. For instance, in the France dataset, the average MAPE value of CEEMDAN-LSTM is 1.72%, while the average MAPE of EMD-LSTM and EEMD-LSTM are 2.43% and 1.89%, respectively. CEEMDAN which is the enhanced version of the EMD and EEMD has a better decomposition ability, and this result is consistent with the conclusion reported in Ref. [42].
4. The proposed CEEMDAN-EWT-LSTM method achieves better performance compared to CEEMDAN-LSTM. The proposed CEEMDAN-EWT-LSTM can enhance the forecasting accuracy of the CEEMDAN-LSTM by more than 17% for both datasets. MAPE values decrease by 17.51% on average in the France dataset and 17.01% in the Turkey dataset, demonstrating the effects of the denoising technique on further improving the accuracy of CEEMDAN-LSTM. By denoising IMF 1 generated from CEEMDAN, the negative impact of randomness and irregularities on IMF 1 can be reduced, which makes IMF 1 more suitable for forecasting and can easily be modeled. It can be concluded that the use of the EWT denoising technique to smooth and denoise IMF 1 can enhance the forecasting accuracy of ultra-short-term wind power forecasts.
5. Among all the forecasting methods, the proposed CEEMDAN-EWT-LSTM method achieves the best forecasting results for both datasets. The average MAPE values of the proposed CEEMDAN-EWT-LSTM method are all less than 1.5% in both datasets. It demonstrates that the proposed method has excellent forecasting ability in ultra-short-term wind power forecasting. The proposed method fully combines the advantage of CEEMDAN decomposition, EWT denoising, and deep learning-LSTM forecasting method, which makes it performs better than other benchmarking methods. The proposed method can decompose the nonstationary and nonlinear wind data into several more relatively stable subseries by using CEEMDAN and further denoise the highest frequency subseries generated from CEEMDAN to achieve higher forecasting accuracy. Therefore, the proposed CEEMDAN-EWT-LSTM method is an effective tool for ultra-short-term wind power forecasting.

4.5. *Time series cross-validation*

In order to obtain a robust measurement of the model's performance, a time series cross-validation scheme [77] was implemented on the France and Turkey datasets. In this study, a 3-fold time series cross-validation scheme was applied to the first four months of the data set (January to April). The 3-fold time series cross-validation scheme is diagrammatically represented in Fig. 8.

The time series cross-validation results for the France and Turkey datasets are presented in Table 5, and the improvement percentages are summarized in Table 6. As seen in Table 5, the lowest error was achieved by the proposed method for both datasets. In terms of the percentage improvement in Table 6, the average improvement percentages of the proposed method achieve up to 67.01% on the France dataset and 78.61% on the Turkey dataset. In summary, the proposed method demonstrates superior forecasting accuracy based on time series cross-validation analysis.

4.6. *Comparative experiments*

In this section, the proposed method is compared with other state-of-the-art methods, namely Empirical Mode Decomposition-Elman Neural Network (EMD-ENN) [35] and Ensemble Empirical Mode Decomposition BO-LSTM Neural Network (EEMD-BO-LSTM) [38]. The comparative experiment is conducted on the Turkey dataset, and our model achieves the best performance, and our proposed method achieves the best performance. The comparative experiment results are presented in Table 7, and the improvement percentages are summarized in Table 8. The comparative experiment results in Table 7 show that our proposed method outperforms both EMD-ENN and EEMD-BO-LSTM, achieving the smallest MAPE, RMSE, and MAE values. Specifically, our proposed method showed an average improvement of 38.30% in MAPE compared to EMD-ENN and a 28.05% improvement compared to EEMD-BO-LSTM. These results demonstrate our proposed method's effectiveness and advantage over existing state-of-the-art methods for the Turkey dataset.

5. Conclusion

Wind power forecasting plays a critical role in ensuring the reliable and efficient operation of the power system. Due to the nonlinear and nonstationary characteristics of wind data, it is difficult to establish wind power forecasts with high accuracy. In this study, a hybrid CEEMDAN-EWT deep learning-based LSTM method is presented to forecast wind power generation. In the proposed method, the CEEMDAN is employed to decompose the original wind power data, and the EWT denoising technique is used to denoise the first IMF generated from the CEEMDAN. Afterward, LSTM is used to forecast all the subseries generated from CEEMDAN-EWT. In the last step, the forecasting results of each subseries are aggregated by summation to obtain the final forecasting results. The performance of the proposed method is validated using real-world data from two wind farms in two different countries. According to the experimental results, the proposed CEEMDAN-EWT-LSTM is superior to other benchmark methods. The proposed method is a promising tool for ultra-short-term wind power forecasting. The scope of the study will be expanded from univariate to multivariate in future research by including relevant factors as input data.

Data availability

The source code and datasets discussed in this manuscript are available at: https://github.com/irenekarijadi/CEEMDAN-EWT-LSTM/

CRediT authorship contribution statement

Irene Karijadi: Conceptualization, Formal analysis, Methodology, Software, Data curation, Validation, Visualization, Writing – original draft. **Shuo-Yan Chou:** Conceptualization, Funding acquisition, Project administration, Supervision, Validation, Writing – review & editing. **Anindhita Dewabharata:** Formal analysis, Data curation, Validation, Writing – review & editing.

Declaration of competing interest

The authors declare that they have no known competing financial interests or personal relationships that could have appeared to influence the work reported in this paper.

Acknowledgement

This research was partially supported by the National Science and Technology Council of the Republic of China (Taiwan) under grant NSTC 111-2923-E-011-004-MY3 and the Taiwan Building Technology Center from The Featured Areas Research Center Program within the framework of the Higher Education Sprout Project by the Ministry of Education in Taiwan.

References

[1] P. Moodley, Sustainable biofuels: opportunities and challenges, Sustain. Biofuel. (2021) 1–20, https://doi.org/10.1016/B978-0-12-820297-5.00003-7.
[2] M. Zerta, P.R. Schmidt, C. Stiller, H. Landinger, Alternative World Energy Outlook (AWEO) and the role of hydrogen in a changing energy landscape, Int. J. Hydrogen Energy 33 (2008), https://doi.org/10.1016/j.ijhydene.2008.01.044.
[3] I.E.A. IEA, Electricity Market Report, Electricity Market Report, 2022.
[4] M.D.A. Al-falahi, S.D.G. Jayasinghe, H. Enshaei, A review on recent size optimization methodologies for standalone solar and wind hybrid renewable energy system, Energy Convers. Manag. 143 (2017), https://doi.org/10.1016/j.enconman.2017.04.019.
[5] A. Suman, Role of renewable energy technologies in climate change adaptation and mitigation: a brief review from Nepal, Renew. Sustain. Energy Rev. 151 (2021), https://doi.org/10.1016/j.rser.2021.111524.
[6] International Renewable Energy Agency, IRENA, Global Energy Transformation: A Roadmap to 2050, 2019, 2019.
[7] D. Gielen, F. Boshell, D. Saygin, M.D. Bazilian, N. Wagner, R. Gorini, The role of renewable energy in the global energy transformation, Energy Strategy Rev. 24 (2019) 38–50, https://doi.org/10.1016/j.esr.2019.01.006.
[8] A. Kisvari, Z. Lin, X. Liu, Wind power forecasting – a data-driven method along with gated recurrent neural network, Renew. Energy 163 (2021), https://doi.org/10.1016/j.renene.2020.10.119.
[9] J. Yang, Q. Liu, X. Li, X. Cui, Overview of wind power in China: status and future, Sustainability (2017) 9, https://doi.org/10.3390/su9081454.
[10] R. Lacal Arantegui, A. Jäger-Waldau, Photovoltaics and wind status in the European union after the Paris agreement, Renew. Sustain. Energy Rev. 81 (2018), https://doi.org/10.1016/j.rser.2017.06.052.
[11] J. Li, S. Zhang, Z. Yang, A wind power forecasting method based on optimized decomposition prediction and error correction, Elec. Power Syst. Res. (2022) 208, https://doi.org/10.1016/j.epsr.2022.107886.
[12] S. Teleke, M.E. Baran, S. Bhattacharya, A.Q. Huang, Optimal control of battery energy storage for wind farm dispatching, IEEE Trans. Energy Convers. 25 (2010), https://doi.org/10.1109/TEC.2010.2041550.
[13] J. Wang, M. Shahidehpour, Z. Li, Security-constrained unit commitment with volatile wind power generation, IEEE Trans. Power Syst. 23 (2008), https://doi.org/10.1109/TPWRS.2008.926719.
[14] X. Kong, X. Wang, M.A. Abdelbaky, X. Liu, K.Y. Lee, Nonlinear MPC for DFIG-based wind power generation under unbalanced grid conditions, Int. J. Electr. Power Energy Syst. 134 (2022), https://doi.org/10.1016/j.ijepes.2021.107416.
[15] X. Kong, L. Ma, C. Wang, S. Guo, M.A. Abdelbaky, X. Liu, K.Y. Lee, Large-scale wind farm control using distributed economic model predictive scheme, Renew. Energy 181 (2022), https://doi.org/10.1016/j.renene.2021.09.048.
[16] M.A. Abdelbaky, X. Liu, D. Jiang, Design and implementation of partial offline fuzzy model-predictive pitch controller for large-scale wind-turbines, Renew. Energy 145 (2020), https://doi.org/10.1016/j.renene.2019.05.074.
[17] Q. Chen, K.A. Folly, Wind power forecasting, IFAC-PapersOnLine 51 (2018), https://doi.org/10.1016/j.ifacol.2018.11.738.
[18] D.Y. Hong, T.Y. Ji, M.S. Li, Q.H. Wu, Ultra-short-term forecast of wind speed and wind power based on morphological high frequency filter and double similarity search algorithm, Int. J. Electr. Power Energy Syst. 104 (2019), https://doi.org/10.1016/j.ijepes.2018.07.061.
[19] J. Jung, R.P. Broadwater, Current status and future advances for wind speed and power forecasting, Renew. Sustain. Energy Rev. 31 (2014), https://doi.org/10.1016/j.rser.2013.12.054.
[20] I. Würth, L. Valldecabres, E. Simon, C. Möhrlen, B. Uzuno glu, C. Gilbert, G. Giebel, D. Schlipf, A. Kaifel, Minute-scale forecasting of wind power—results from the collaborative workshop of IEA Wind task 32 and 36, Energies 12 (2019), https://doi.org/10.3390/en12040712.
[21] R. Liu, M. Peng, X. Xiao, Ultra-short-term wind power prediction based on multivariate phase space reconstruction and multivariate linear regression, Energies 11 (2018), https://doi.org/10.3390/en11102763.
[22] S.S. Soman, H. Zareipour, O. Malik, P. Mandal, A review of wind power and wind speed forecasting methods with different time horizons, in: North American Power Symposium 2010, NAPS, 2010, https://doi.org/10.1109/NAPS.2010.5619586, 2010.
[23] B.M. Hodge, A. Zeiler, D. Brooks, G. Blau, J. Pekny, G. Reklatis, Improved Wind Power Forecasting with ARIMA Models, 2011, https://doi.org/10.1016/B978-0-444-54298-4.50136-7.
[24] K. Methaprayoon, C. Yingvivatanapong, W.J. Lee, J.R. Liao, An integration of ANN wind power estimation into unit commitment considering the forecasting uncertainty, IEEE Trans. Ind. Appl. 43 (2007), https://doi.org/10.1109/TIA.2007.908203.
[25] Y. Kassa, J.H. Zhang, D.H. Zheng, D. Wei, A GA BP hybrid algorithm based ANN model for wind power prediction, in: 2016 4th IEEE International Conference on Smart Energy Grid Engineering, SEGE, 2016, https://doi.org/10.1109/SEGE.2016.7589518, 2016.
[26] E.E. Elattar, Short term wind power prediction using evolutionary optimized local support vector regression, in: IEEE PES Innovative Smart Grid Technologies Conference Europe, 2011, https://doi.org/10.1109/ISGTEurope.2011.6162629.
[27] Y. Wang, D. Wang, Wind power prediction based on the clustered combination of ARMA and PSO-SVM methods, in: ISPEC 2019 - 2019 IEEE Sustainable Power and Energy Conference: Grid Modernization for Energy Revolution, Proceedings, 2019, https://doi.org/10.1109/iSPEC48194.2019.8975127.
[28] A. Lahouar, J. ben Hadj Slama, Hour-ahead wind power forecast based on random forests, Renew. Energy 109 (2017), https://doi.org/10.1016/j.renene.2017.03.064.
[29] Y. Wang, R. Zou, F. Liu, L. Zhang, Q. Liu, A review of wind speed and wind power forecasting with deep neural networks, Appl. Energy 304 (2021), https://doi.org/10.1016/j.apenergy.2021.117766.
[30] Y. Liu, L. Guan, C. Hou, H. Han, Z. Liu, Y. Sun, M. Zheng, Wind power short-term prediction based on LSTM and discrete wavelet transform, Appl. Sci. 9 (2019), https://doi.org/10.3390/app9061108.
[31] J. Zhang, X. Jiang, X. Chen, X. Li, D. Guo, L. Cui, Wind power generation prediction based on LSTM, in: ACM International Conference Proceeding Series, 2019, https://doi.org/10.1145/3325730.3325735.
[32] G. Mu, M. Yang, D. Wang, G. Yan, Y. Qi, Spatial dispersion of wind speeds and its influence on the forecasting error of wind power in a wind farm, J. Modern Power Sys. Clean Ener. 4 (2016), https://doi.org/10.1007/s40565-015-0151-x.
[33] Z. Peng, S. Peng, L. Fu, B. Lu, J. Tang, K. Wang, W. Li, A novel deep learning ensemble model with data denoising for short-term wind speed forecasting, Energy Convers. Manag. 207 (2020), https://doi.org/10.1016/j.enconman.2020.112524.
[34] Z.-W. Zheng, Y.-Y. Chen, X.-W. Zhou, M.-M. Huo, B. Zhao, M.-Y. Guo, Short-term wind power forecasting using empirical mode decomposition and RBFNN, Int. J. Smart Grid Clean Energy 2 (2013) 192–199, https://doi.org/10.12720/sgce.2.2.192-199.
[35] J. Wang, W. Zhang, Y. Li, J. Wang, Z. Dang, Forecasting wind speed using empirical mode decomposition and Elman neural network, Appl. Soft Comput. J. 23 (2014), https://doi.org/10.1016/j.asoc.2014.06.027.
[36] Y. He, Y. Wang, Short-term wind power prediction based on EEMD–LASSO–QRNN model, Appl. Soft Comput. 105 (2021), https://doi.org/10.1016/j.asoc.2021.107288.
[37] Y. Ding, Z. Chen, H. Zhang, X. Wang, Y. Guo, A short-term wind power prediction model based on CEEMD and WOA-KELM, Renew. Energy 189 (2022), https://doi.org/10.1016/j.renene.2022.02.108.
[38] W. Hu, Y. He, Z. Liu, J. Tan, M. Yang, J. Chen, Toward a digital twin: time series prediction based on a hybrid ensemble empirical mode decomposition and BO-LSTM neural networks, J. Mech. Design, Trans. ASME 143 (2021), https://doi.org/10.1115/1.4048414.
[39] Q. Zhang, Z. Tang, S. Cao, G. Wang, Wind farm wind power prediction method based on CEEMDAN and de optimized DNN neural network, in: Proceedings - 2019 Chinese Automation Congress, CAC, 2019, https://doi.org/10.1109/CAC48633.2019.8996744, 2019.
[40] Z. Xing, B. Qu, Y. Liu, Z. Chen, Comparative study of reformed neural network based short-term wind power forecasting models, IET Renew. Power Gener. 16 (2022), https://doi.org/10.1049/rpg2.12384.
[41] Y. Zhang, Y. Chen, Application of hybrid model based on CEEMDAN, SVD, PSO to wind energy prediction, Environ. Sci. Pollut. Control Ser. 29 (2022), https://doi.org/10.1007/s11356-021-16997-3.
[42] Y. Ren, P.N. Suganthan, N. Srikanth, A comparative study of empirical mode decomposition-based short-term wind speed forecasting methods, IEEE Trans. Sustain. Energy 6 (2015), https://doi.org/10.1109/TSTE.2014.2365580.
[43] P. Lv, Y. Shu, J. Xu, Q. Wu, Modal decomposition-based hybrid model for stock index prediction, Expert Syst. Appl. 202 (2022), 117252, https://doi.org/10.1016/J.ESWA.2022.117252.

[44] Y. Lin, Z. Lin, Y. Liao, Y. Li, J. Xu, Y. Yan, Forecasting the realized volatility of stock price index: a hybrid model integrating CEEMDAN and LSTM, Expert Syst. Appl. 206 (2022), 117736, https://doi.org/10.1016/J.ESWA.2022.117736.
[45] S.N. Chegini, A. Bagheri, F. Najafi, Application of a new EWT-based denoising technique in bearing fault diagnosis, Measurement 144 (2019), https://doi.org/10.1016/j.measurement.2019.05.049.
[46] Y. Song, S. Zeng, J. Ma, J. Guo, A fault diagnosis method for roller bearing based on empirical wavelet transform decomposition with adaptive empirical mode segmentation, Measurement 117 (2018), https://doi.org/10.1016/j.measurement.2017.12.029.
[47] O. Singh, R.K. Sunkaria, ECG signal denoising via empirical wavelet transform, Australas. Phys. Eng. Sci. Med. 40 (2017), https://doi.org/10.1007/s13246-016-0510-6.
[48] W. Liu, S. Cao, Y. Chen, Seismic time-frequency analysis via empirical wavelet transform, Geosci. Rem. Sens. Lett. IEEE 13 (2016), https://doi.org/10.1109/LGRS.2015.2493198.
[49] J. Hu, J. Wang, K. Ma, A hybrid technique for short-term wind speed prediction, Energy 81 (2015), https://doi.org/10.1016/j.energy.2014.12.074.
[50] J. Hu, J. Wang, Short-term wind speed prediction using empirical wavelet transform and Gaussian process regression, Energy 93 (2015), https://doi.org/10.1016/j.energy.2015.10.041.
[51] J. Hu, J. Wang, L. Xiao, A hybrid approach based on the Gaussian process with t-observation model for short-term wind speed forecasts, Renew. Energy 114 (2017), https://doi.org/10.1016/j.renene.2017.05.093.
[52] W. Zeng, Y. Cao, L. Feng, J. Fan, M. Zhong, W. Mo, Z. Tan, Hybrid CEEMDAN-DBN-ELM for online DGA serials and transformer status forecasting, Elec. Power Syst. Res. 217 (2023), 109176, https://doi.org/10.1016/J.EPSR.2023.109176.
[53] N.E. Huang, Z. Shen, S.R. Long, M.C. Wu, H.H. Shih, N. Yen, C.C. Tung, H.H. Liu, The Empirical Mode Decomposition and the Hilbert Spectrum for Nonlinear and Non-stationary Time Series Analysis, Proceedings of the Royal Society A, 1996, p. 454.
[54] L. Yang, J. Cai, A method to identify wet ball mill's load based on CEEMDAN, RCMDE and SRNN classification, Miner. Eng. 165 (2021), https://doi.org/10.1016/j.mineng.2021.106852.
[55] K. Barnova, R. Kahankova, R. Jaros, M. Litschmannova, R. Martinek, A comparative study of single-channel signal processing methods in fetal phonocardiography, PLoS One 17 (2022), https://doi.org/10.1371/journal.pone.0269884.
[56] D.O. Afanasyev, E.A. Fedorova, The long-term trends on the electricity markets: comparison of empirical mode and wavelet decompositions, Energy Econ. 56 (2016), https://doi.org/10.1016/j.eneco.2016.04.009.
[57] D.O. Afanasyev, E.A. Fedorova, The long-term trends on the electricity markets: comparison of empirical mode and wavelet decompositions, Energy Econ. 56 (2016), https://doi.org/10.1016/j.eneco.2016.04.009.
[58] D. Shu-wen, L. Lu-jun, W. Qing-qu, W. Kang-le, C. Peng-zhan, Fiber optic gyro noise reduction based on hybrid CEEMDAN-LWT method, Measurement 161 (2020), https://doi.org/10.1016/j.measurement.2020.107865.
[59] M.E. Torres, M.A. Colominas, G. Schlotthauer, P. Flandrin, A complete ensemble empirical mode decomposition with adaptive noise, in: ICASSP, IEEE International Conference on Acoustics, Speech and Signal Processing - Proceedings, 2011, https://doi.org/10.1109/ICASSP.2011.5947265.
[60] O. Singh, R.K. Sunkaria, An empirical wavelet transform based approach for multivariate data processing application to cardiovascular physiological signals, Bio. Algorithm Med. Syst. 14 (2018), https://doi.org/10.1515/bams-2018-0030.
[61] W. Liu, W. Chen, Recent advancements in empirical wavelet transform and its applications, IEEE Access 7 (2019), https://doi.org/10.1109/ACCESS.2019.2930529.
[62] J. Gilles, Empirical wavelet transform, IEEE Trans. Signal Process. 61 (2013), https://doi.org/10.1109/TSP.2013.2265222.
[63] Y. Xu, K. Zhang, C. Ma, Z. Sheng, H. Shen, An adaptive spectrum segmentation method to optimize empirical wavelet transform for rolling bearings fault diagnosis, IEEE Access 7 (2019), https://doi.org/10.1109/ACCESS.2019.2902645.
[64] T. Fischer, C. Krauss, Deep learning with long short-term memory networks for financial market predictions, Eur. J. Oper. Res. 270 (2018), https://doi.org/10.1016/j.ejor.2017.11.054.
[65] J. Ren, Z. Yu, G. Gao, G. Yu, J. Yu, A CNN-LSTM-LightGBM based short-term wind power prediction method based on attention mechanism, Energy Rep. 8 (2022) 437–443, https://doi.org/10.1016/J.EGYR.2022.02.206.
[66] Y. Yu, X. Si, C. Hu, J. Zhang, A review of recurrent neural networks: lstm cells and network architectures, Neural Comput. 31 (2019), https://doi.org/10.1162/neco_a_01199.
[67] D. Hládek, J. Staš, S. Ondáš, Comparison of Recurrent Neural Networks for Slovak Punctuation Restoration; Comparison of Recurrent Neural Networks for Slovak Punctuation Restoration, 2019. https://keras.io/.
[68] P. Lu, L. Ye, M. Pei, Y. Zhao, B. Dai, Z. Li, Short-term wind power forecasting based on meteorological feature extraction and optimization strategy, Renew. Energy 184 (2022) 642–661, https://doi.org/10.1016/J.RENENE.2021.11.072.
[69] L. Xiang, J. Liu, X. Yang, A. Hu, H. Su, Ultra-short term wind power prediction applying a novel model named SATCN-LSTM, Energy Convers. Manag. 252 (2022), 115036, https://doi.org/10.1016/J.ENCONMAN.2021.115036.
[70] J. Wei, X. Wu, T. Yang, R. Jiao, Ultra-short-term forecasting of wind power based on multi-task learning and LSTM, Int. J. Electr. Power Energy Syst. 149 (2023), https://doi.org/10.1016/j.ijepes.2023.109073.
[71] Y. Li, Y. Li, X. Chen, J. Yu, H. Yang, L. Wang, A new underwater acoustic signal denoising technique based on CEEMDAN, mutual information, permutation entropy, and wavelet threshold denoising, Entropy 20 (2018), https://doi.org/10.3390/e20080563.
[72] M. Sun, Q. Li, P. Lin, Short-term stock price forecasting based on an SVD-LSTM model, Intel. Automat. &; Soft Comput. 28 (2021), https://doi.org/10.32604/iasc.2021.014962.
[73] Y. Shi, L. Zhang, S. Lu, Q. Liu, Short-term demand prediction of shared bikes based on LSTM network, Electronics 12 (2023), https://doi.org/10.3390/electronics12061381.
[74] Y. He, Y. Wang, Short-term wind power prediction based on EEMD–LASSO–QRNN model, Appl. Soft Comput. 105 (2021), https://doi.org/10.1016/j.asoc.2021.107288.
[75] H. Liu, C. Yu, H. Wu, Z. Duan, G. Yan, A new hybrid ensemble deep reinforcement learning model for wind speed short term forecasting, Energy 202 (2020), https://doi.org/10.1016/j.energy.2020.117794.
[76] Y. Jiang, S. Liu, N. Zhao, J. Xin, B. Wu, Short-term wind speed prediction using time varying filter-based empirical mode decomposition and group method of data handling-based hybrid model, Energy Convers. Manag. 220 (2020), https://doi.org/10.1016/j.enconman.2020.113076.
[77] F. Senesoulin, I. Ngamroo, S. Dechanupaprittha, Estimation of dominant power oscillation modes based on ConvLSTM approach using synchrophasor data and cross-validation technique, Sustain. Energy, Grids Net. 31 (2022), 100731, https://doi.org/10.1016/J.SEGAN.2022.100731.